Title
MOLECULAR CHARACTERIZATION OF NICKEL AND VANADIUM NON-PORPHYRIN COMPOUNDS FOUND IN HEAVY CRUDE PETROLEUMS AND BITUMENS

Authors

Fish, R.H.
Reynolds, J.G.
Gallegos, E.J.

Publication Date

1986-11-01

Lawrence Berkeley Laboratory
UNIVERSITY OF CALIFORNIA

APPLIED SCIENCE DIVISION

Presented at the 191st ACS Meeting, Division
of Geochemistry, New York, NY, April 13-18, 1986;
and to be published in the Proceedings

MOLECULAR CHARACTERIZATION OF NICKEL AND VANADIUM NON-PORPHYRIN COMPOUNDS FOUND IN HEAVY CRUDE PETROLEUMS AND BITUMENS

R.H. Fish, J.G. Reynolds, and E.J. Gallegos

November 1986

APPLIED SCIENCE
DIVISION

Prepared for the U.S. Department of Energy under Contract DE-AC03-76SF00098

DISCLAIMER

MOLECULAR CHARACTERIZATION OF NICKEL AND VANADIUM NONPORPHYRIN COMPOUNDS FOUND IN HEAVY CRUDE PETROLEUMS AND BITUMENS

*Richard H. Fish**
Lawrence Berkeley Laboratory,
University of California,
Berkeley, California 94720

John G. Reynolds and Emilio J. Gallegos,
Chevron Research Company,
Richmond, California 94802

Pyridine/water extracts of selected crude petroleums were separated by polarity on a high performance liquid chromatography (HPLC) octadecylsilane column (ODS) into three fractions; low, moderate, and high polar. The moderate and low polar fractions were examined by electron impact mass spectroscopy (EIMS) to elucidate structural and behavioral characteristics of vanadyl petroporphyrin and metallo-nonporphyrin compounds. The EIMS results indicated vanadyl petroporphyrins in Cerro Negro and Wilmington moderate polar fractions and possibly in the Wilmington low polar fraction. These EIMS results showed the presence of petroporphyrins in the above-mentioned fractions, but no discrete information about the metallo-nonporphyrins.

A highly polar nickel fraction from a Wilmington crude petroleum pyridine/water extract, separated on the ODS column, was further purified on a cyano normal phase column. This fraction had a nickel concentration of approximately 15,000 wppm, and was examined by EIMS mass spectroscopy. The spectral results indicated several homologous series structures possible for the binding sites of nickel. Further examination of the same fraction by positive ion fast atom bombardment (FAB+) mass spectroscopy, using a metal ion exchange technique, showed a substantially simplified spectrum and indicated the possibility of the nickel binding sites being small molecular weight naphthenic (carboxylic) acid salts.

Gilsonite, a bitumen, was analyzed by reversed-phase HPLC with graphite furnace atomic absorption (RP-HPLC-GFAA) element specific detection, which indicated that the nickel is predominantly bound as metallopetroporphyrin, while a small portion eluted as a highly polar metallo-nonporphyrin fraction.

These results are important in the identification of nonporphyrin metal-containing compounds in heavy crude petroleums and residua and could be beneficial for future petroleum exploration as metallobiomarkers.

We have extensively examined various crude petroleums and separated fractions to determine the characteristics of the metal-containing compounds, particularly the metallononporphyrins. Recently, we reported the molecular weights (MW) of the vanadium and nickel compounds found in selected heavy crude petroleums -- Boscan, Cerro Negro, Wilmington, and Prudhoe Bay -- and their extracts *(1,2)* by size exclusion chromatography in conjunction with graphite furnace atomic absorption selective metal detection (SEC-HPLC-GFAA). The metals distribution was found to be unique for each petroleum, while the histogrammic metals profiles may have utility for fingerprinting the heavy crude petroleums. In the case of vanadium, the majority of the metal-containing compounds falls into the 2,000 to 9,000 dalton MW range, while 3 to 7% was found in the MW range > 9,000 daltons. The low MW range was calibrated by vanadyl and nickel model compounds, with 23 to 30% having a MW range of <400 daltons. Although these molecular weights may be exaggerated in the high MW range *(3,4)*, we feel this low MW range result provides strong evidence for the metallo-nonporphyrin coordination sphere.

Pyridine/water extractions have been applied to the same heavy crude petroleums for further identification of these metal-containing molecules *(2)*. The extraction procedure removes metal-containing compounds from all molecular weight ranges, placing the compounds in the size range of vanadyl and nickel model compounds. As well, 40 to 80% of the vanadium comes from the MW range >2,000 daltons. The extract consists predominantly of very small MW compounds with an average MW of approximately 350 daltons. By comparison with nickel and vanadyl model compounds of similar MW, we also feel this further substantiates metallo-nonporphyrin coordination spheres.

These pyridine/water extracts were separated by RP-HPLC into three fractions based on polarity, and the fractions were monitored by element specific detection (GFAA) and UV-vis spectroscopy *(2)*. Most of the nickel-containing compounds eluted in the most polar fractions. Comparison with model compound retention times indicated these compounds are nonporphyrin bound. Most of the vanadium-containing compounds were found in the moderate polar fractions. Rapid scan (RS) UV-vis data showed a prominent Soret band in this fraction for Boscan and Cerro Negro indicating at least some of the vanadium is bound as petroporphyrin. This was not the case for Wilmington and Prudhoe Bay moderate polar fractions where the RS-UV-vis exhibited little or no Soret. At this time, we have no adequate model compounds that co-elute in this fraction. The least polar fraction also contained vanadium (up to 30% of total in crude). Model compound retention times showed the model porphyrins eluted in this fraction, but the absence of a prominent Soret in this fraction for most of the crudes suggests nonporphyrins.

The moderate and low polar RP-HPLC fractions from Boscan, Cerro Negro, Wilmington, and Prudhoe Bay crude petroleums, were examined by electron paramagnetic resonance (EPR) spectroscopy to further elucidate the structure of the average coordination sphere around the vanadium-containing molecules *(5)*. Several nonporphyrin coordination spheres for the vanadyl ion were observed: 1) Boscan moderate polar and Prudhoe Bay moderate and low polar fractions exhibited N_2S_2 coordination. 2) Cerro Negro and Wilmington moderate polar fractions showed S_4 coordination. 3) Boscan low polar fraction showed N_4 coordination. 4) Cerro Negro had distinctively different parameters showing a NOS_2 coordination.

We have also examined the RP-HPLC fractions by EIMS to further identify the metallo-nonporphyrin components. Unfortunately, the EIMS spectral studies only revealed the presence of metallopetroporphyrins in certain fractions. The metallo-nonporphyrins remained undifferentiated in the organic matrix.

We have attempted to elucidate the structure of nickel-containing molecules in the high polar RP-HPLC fractions by using C-18 ODS reversed-phase and cyano normal phase chromatography techniques to purify the pyridine/water extract of Wilmington crude petroleum. We have examined the resulting purified fractions with EIMS, FAB+, and metal replacement FAB+ mass spectroscopies. We have also attempted to verify the existence of these highly polar nickel components in other carbonaceous materials. For example, we examined Gilsonite by RP-HPLC-GFAA and found this highly polar nickel complexes may also be present in this petroleum precursor.

Results and Discussion

Spectral Analyses of the Moderate and Low Polar RP-HPLC Fractions. In efforts to identify the elusive nonporphyrin metal-containing species, the moderate and low polar fractions, obtained by the RP-HPLC separation of the pyridine/water extracts of Boscan, Cerro Negro, Prudhoe Bay and Wilmington crude petroleums, were examined by EPR, EIMS, and RS-UV-vis spectroscopies. The EPR techniques employed utilize vanadyl square pyramidal model compounds to elucidate the average first coordination sphere of the vanadium-containing compounds in the sample studied *(6-10)*. The EPR *(5)* and RS-UV-vis *(1,2)* results have been reported elsewhere.

The EIMS of the RP-HPLC fractions, in general, identified the existence of vanadyl petroporphyrins when present. Figure 1 shows the EIMS for Cerro Negro moderate polar fraction for m/z of 200 to 800. Although some individual peaks stand out, the vanadyl etio homologous series is evident from m/z of 473 to 557. The vanadyl deoxophylloerythroetio (DPEP) homologous series, although less prominent, is evident from m/z of 499 to 575.

The same spectral characteristics were observed in the Wilmington moderate polar fraction indicating vanadyl petroporphyrins. RS-UV-vis examination of these moderate polar fractions also indicated the presence of vanadyl petroporphyrins by the appearance of the distinctive 408 nm Soret band *(1,2)*.

The vanadyl porphyrin model compounds elute in the low polar fraction. We do not have model compounds with a Soret at 408 nm which co-elute in the moderate polar fraction. These could represent metallopetroporphyrins with a carboxylic acid functionality, *(11,12)* dimers of petroporphyrins *(13,14)*, or petroporphyrins of much higher molecular weight *(15)*.

These EIMS results do not necessarily conflict with the EPR data for these fractions which showed N_2S_2 average first coordination sphere around the vanadyl ion *(5)*. The EPR techniques are average parameter techniques and would not necessarily be able to resolve a minor percentage of the N_4 coordination sphere. The EIMS method also only detects the petroporphyrins, but does not quantitate them.

The EIMS spectrum of Prudhoe Bay low polar fraction, Figure 2, shows no metallopetroporphyrin homologous series. This spectrum is very typical of those fractions which contained no discernible petroporphyrins. As can be seen by Figure 2, any individual homologous series are overwhelmed by the organic matrix. The same spectral characteristics were observed for Boscan and Cerro Negro low polar fractions indicating very low levels or no petroporphyrins. This is corroborated by only a weak 408 nm Soret found by RS-UV-vis.

The EPR of these fractions indicated N_4 coordination for the Boscan and Prudhoe Bay low polar fractions and NOS_2 coordination for the Cerro Negro low polar fraction. The N_4 nonporphyrin coordination sphere has been seen before in the EPR studies and suggests a variety of nonporphyrin ligand structures (5,16,17).

Purification of the Highly Polar Nickel Compounds Found in Wilmington Heavy Crude Petroleum. RP-HPLC-GFAA examination of the pyridine/water extracts of several heavy crude petroleums indicated the majority of the nickel-containing compounds eluted in the high polar fraction. The lack of EIMS spectral identification of these fractions suggested the need for further purification.

Wilmington crude petroleum was extracted with pyridine/water and the extract was separated on the ODS column into a highly polar fraction (methanol eluted) and a less polar fraction (methylene chloride eluted). The highly polar fraction was rechromatographed on the ODS column, and was found to increase its nickel concentration from 8000 to 11000 wppm. Table I shows the concentrations of these fractions.

Further purification was performed on a cyano column using a methylene chloride to methanol solvent gradient. The use of bonded phase HPLC separations, either reversed-phase or cyano columns, offer several unique advantages over the more conventional silica columns *(18)*. Because polar solvents can be used, bonded packings are capable of separating highly polar metal-containing complexes. These highly polar complexes would be irreversibly bonded to silica, because silica packings rapidly degrade in polar solvents. Reversed-phase packings allow for partition separations where the more polar components elute first. Cyano columns can be operated in normal or reversed-phase modes providing increased flexibility over silica columns.

Table I: Nickel Concentrations of Preparatively Collected Fractions from the Wilmington Petroleum Extract[1]

	ODS I	ODS II[2]	Cyano Peak I[3]
Ni, (ppm)	8,040	11,000	14,250
Wt. of Collected fraction, (mg)	60	25.2	4.0
Nickel Complexes, (wt %)[4]	4.1	5.7	7.4

[1] Concentrations Determined Using Aqua Regia Conditions and Standards Plots
[2] Rechromatography of ODS I Using ODS Column
[3] Rechromatography of ODS II Using Cyano Column
[4] Assumed Molecular Weight of Complexes 300 - Daltons

Figure 3 shows the elution profile for this separation with the effluent monitored for both UV-vis wavelength of 254 nm, and GFAA wavelength of 232 nm. Organic impurities eluted quickly at approximately 3 minutes. Two fractions of nickel complexes eluted; the first in the 50% methylene chloride solvent mixture. This corresponded to several sharp maxima in the UV-vis monitor. A second fraction eluted shortly after the solvent system was changed to 100% methanol. This fraction corresponded to a broader maximum in the UV-vis monitor. These nickel compounds are more polar than the nickel nonporphyrin model complexes which eluted at approximately 10 percent methanol. In contrast, nickel (II) chloride eluted at approximately 28 minutes, which is substantially longer than the second nickel fraction in Figure 3 and precludes the possibility of inorganic nickel.

Table I shows the further concentration of the nickel fraction by chromatography on a cyano column and this corresponds to 7.4 wt % nickel complex in the sample (assuming an average molecular weight of 300 daltons based on model compound elution times from SEC-HPLC-GFAA studies).

Mass Spectral Analyses of the Cyano Column Separated Nickel Fraction. In order to interpret the mass spectral results of the fraction derived from the cyano column separation, we examined in detail, the mass spectral *(19)* behavior of several nickel and vanadium model compounds by EIMS, FAB, field ionization and field desorption (FI/FD), and chemical ionization (CI) in positive or negative ionization modes.

Figure 4 shows nickel (II) bis(diethyldithiocarbamate), nickel (II) tetramethyldibenzotetraaza-[14]-annulene (TADA), and nickel (II) bis(dipivaloylmethane) (DPM) by EIMS. All three parent ions are observable at *m/z* 354, 400, and 424 respectively. Even though the parent ion is the dominant ion, for the dithiocarbamate complex, the spectrum is complicated by substantial fragmentation. This extensive fragmentation is not evident for the other model compounds, but the $Ni(DPM)_2$ spectrum shows a fragment ion to be the dominant peak. While these spectra give identifiable patterns, they do not exhibit any systematic behavior. Interpretation of unknown species can be substantially complicated by the lack of systematic behavior, and we do not necessarily expect to identify the metallo-nonporphyrin compounds by this method.

Thin layer and RP-HPLC chromatography indicated that nickel carboxylate model compounds have a very similar polarity behavior, when compared to these concentrated nickel fractions. Because this is the case, nickel carboxylates were selected as model compounds. Carboxylic acids are appropriate choices because they have been detected and characterized in carbonaceous materials and can constitute up to 3 wt % of the crude petroleum *(20)*.

We also examined nickel acetate, nickel bis(2-ethylhexanoate), and a naphthenic acid extract from crude petroleum in which the nickel was synthetically placed. Figure 5 shows the EIMS of the nickel naphthenates. Clearly, the parent ion homologous series is evident in the spectrum. The naphthenates show even mass molecular ions extending from about m/z 426 to 582. Note, though, the intensity of the molecular ions is substantially less than that of the major fragments. The presence of impurities would easily overwhelm the parent ions, causing substantial interpretation problem in mixtures.

The cyano column purified nickel fractions of the Wilmington crude petroleum extract were combined and examined by EIMS and compared to the spectra of the nickel model compounds. The spectrum of the purified nickel fraction is shown in Figure 6. Unfortunately, as expected from the complicated spectrum of the nickel naphthenates, no clearly defined metallo-nonporphyrin species are identifiable. Several homologous series are discernible, but their association with nickel is tenuous.

The cyano column purified nickel fraction was also examined by EIMS for metallopetroporphyrins at m/z values where porphyrins should be detected (not shown). At the concentration of nickel in this sample, the petroporphyrins would be overwhelmingly evident; however, no porphyrins were detected. Thus, it is evident that these compounds are not metallopetroporphyrins.

Positive Ion Fast Atom Bombardment (FAB+) Mass Spectroscopic Analyses of the Cyano Column HPLC Fractions. FAB+ is a particularly efficient method for examining polar components in hydrocarbon mixtures. The technique allows the observation of the polar portion of a sample without the complication of the neutral organic components (these are not observed by the FAB+ technique), and greatly simplifies analyses of the spectra. In addition, only certain ionic species are observable, i.e., vanadium and nickel complexes do not show ligand-metal ions, while calcium, magnesium, silver, and iron do show these ions. In addition, only certain metal complexes are also seen, e.g., porphyrins and acetylacetonates are not necessarily observed, while carboxylic acid complexes are observed.

Several carboxylic acid model compounds were examined by FAB+. Nickel (II) bis(2-ethylhexanoate) was examined using triethanolamine (TEA) as the hydrogen source. Although some fragments of the acid are apparent in the spectrum (not shown), the parent ions necessary for identification of the model compound are not present in high enough concentration to be evident. Fragments of Ni + TEA are also evident. In the FAB+ spectrum, the metal ion fragments from the complex are detected, but the ligands are not apparent. Figure 7 shows the FAB+ spectrum of nickel naphthenates and TEA, which also gave reasonable EIMS spectra (Figure 5). The metal-ligand parent ions are not obvious; however, Ni + TEA ions are evident. Although the technique is not viable for ligand identification, it may have utility for metal ion identification.

Recent developments *(21)* have shown, using calcium compounds with a FAB+ ion source, well resolved spectra of naphthenic (carboxylic) acids. This technique exchanges the metal ion of the complex with calcium and gives a calcium naphthenate ion spectrum. Figure 8 shows the FAB+ spectrum of the nickel naphthenate mixture with TEA and calcium acetate. Several homologous series of carboxylic acids + Ca + TEA are apparent in the spectrum. (FAB- shows the naphthenic acid series with a maximum at *m/z* of 251.) These match identically to FAB+ spectra of calcium naphthenates synthetically prepared from the same naphthenic acid source. The FAB+ results of several carboxylic acid model compounds of different metals also responded similarly with calcium compounds and TEA. The results of these experiments and the development of the technique will be published elsewhere *(21)*.

The cyano column purified nickel fraction from the Wilmington crude petroleum extract was examined by the FAB+ metal exchange technique. The FAB+ spectrum of the fraction with just TEA shows no apparent parent ions, just the $Ni(TEA)_2$ ion. This feature was also common to model compound spectra. Figure 9 shows the corresponding FAB+ spectrum with Ca and TEA. Apparently, there are several homologous series of nickel compounds that are thought to be carboxylic acids complexes. In addition, detailed examination of the spectrum further shows that carboxylic acids are possible binding sites for the nickel, when compared to the EIMS spectrum of the same material (Figure 6).

Reactions *1* through *8* are presumed to take place as the calcium and TEA doped with the nickel fraction is bombarded with krypton neutral atoms in the fast atom bombardment process. These reactions explain most of the ions observed in the metal atom exchange technique. The mechanism of this exchange has not been elucidated, but the nickel appears to be removed, and the calcium complex is formed with only one carboxylic acid ligand. The other coordination site on the calcium is taken with a TEA fragment (this adds *m/z* of 189 to the free acid parent fragment).

$$(RCO_2)_2Ni + TEA + Ca^{2+} \rightarrow \left[RCO_2CaTEA\right]^+ \qquad (1)$$

$$\rightarrow \left[RCO_2Ca_2TEA_2\right]^+ \qquad (2)$$

$$\rightarrow \left[(NiTEA)_2\right]^+ \qquad (3)$$

m/z 411

$$\rightarrow \left[(CaTEA)_2\right]^+ \qquad (4)$$

m/z 375

$$\rightarrow \left[NiTEA_2\right]^+ \qquad (5)$$

m/z 355

$$\rightarrow \left[CaTEA_2\right]^+ \qquad (6)$$

m/z 337

$$\rightarrow \left[NiTEA\right]^+ \qquad (7)$$

m/z 206

$$\rightarrow \left[CaTEA\right]^+ \qquad (8)$$

m/z 188

The acid molecular weight can be ascertained from the EIMS of the sample. In the EIMS, the intensity of the metal-containing molecular ion is about 1/200 of the fragments. As a result, when comparing the FAB+ spectrum to the EIMS spectrum of the same material, one must look for the acid anion in the EIMS spectrum, not the nickel complex.

In Figure 9, three homologous series are clearly indicated with the possibility of several more. The corresponding carboxylic acid fragment, as observed in the EIMS spectrum (Figure 6) of the sample, are indicated in parentheses above the corresponding metal-ligand peak. The homologous series in the FAB+ spectrum starting at m/z 422 could correspond to the EIMS series starting at m/z 233. This series is apparent in the EIMS figure on the lower right side of the massive peak (m/z 373 and 359). This could be attributed to four ring saturated naphthenic acids. Likewise, the homologous series starting at m/z 410 in the FAB+ spectrum possibly correlates with three ring saturated naphthenic acids, and the series starting at m/z 440 corresponds to two ring saturated naphthenic acids.

The two most intense peaks in Figure 9 correspond to the C20 four ring saturated acid at m/z 506 and the C15 four ring saturated acid at m/z 436 and can be related by an isoprene unit (C5). This suggests the two, three, four, and five ring components are due to bicyclic sesquiterpanoic, tricyclic diterpanoic, and four and five ring triterpanoic (steranoic and hopanoic) acids. Figure 10 shows generalized structures of these acid ligands. Model compound data, by the metal replacement technique, also indicates replacement reactions as shown in reaction 2. This reaction adds another 187 mass units to the molecule. Although, peaks corresponding to the homologous series formed by reaction 2 can be located in the FAB+ spectrum (not shown), the noise inhibits any clear identification of these species.

RP-HPLC-GFAA Studies on Gilsonite. Gilsonite, a bitumen (Eocene, Unita Basin, Utah), has a high concentration of nickel (100 wppm), but a low concentration of vanadium. We chose Gilsonite as another possible source of the highly polar nickel compounds, because it already had been examined for petroporphyrins *(22)*. In addition, Gilsonite is associated with the Green River Formation and has petroporphyrins which should have experienced mild thermal alterations. Thus, we wanted to ascertain whether the presumed nickel carboxylates in Wilmington crude petroleum were present in Gilsonite.

Gilsonite was dissolved in THF and separated on the C-18 ODS column and the effluent monitored by GFAA. Figure 11 shows the nickel RP-HPLC-GFAA profile of the column effluent, which was also monitored at 320 and 408 nm. Three different component classes containing nickel were separated: compounds eluting at 1) the solvent front, 2) 24 minutes (80% THF), and 3) 36 minutes (100% THF). The most polar nickel components eluted at the solvent front, but are in minor amounts compared to other bands. The middle fraction eluted at the same time as nickel etioporphyrin. The 408 nm response also indicates that at least some of these compounds are porphyrins. We did not have standards which elute at the same time as the third fraction (36 min). The prominent Soret indicates these are petroporphyrin components. Unfortunately, we have not been able to obtain the needed concentrations of this highly polar nickel compound fraction to verify the metal-containing components by FAB+ as nickel carboxylates. However, we speculate that these are small amounts of nickel carboxylates in Gilsonite, which are potential conduits for nickelation of porphyrin ligands during fossilization.

Conclusion

We have separated pyridine/water extracts of selected crude petroleums by reversed-phase chromatography, and examined the vanadium-containing compounds in the moderate and low polar fractions by mass spectroscopy. The EIMS results indicated vanadyl petroporphyrins in Cerro Negro and Wilmington moderate polar fraction and possibly in the

Wilmington low polar fraction. The EIMS results provided no additional information on the metallo-nonporphyrins.

By further purification of the highly polar fraction from the ODS separation of the Wilmington crude petroleum extract, we have seen evidence of bonding for at least one type of nickel-containing nonporphyrin compound. EIMS and FAB+ with metal exchange indicates this nickel is bound as carboxylates (naphthenates).

We are continuing our molecular characterization studies in order to further determine the highly polar nickel compounds as carboxylic salts and as well in our attempts to identify the vanadyl nonporphyrin compounds found in heavy crude petroleums and their precursors.

Experimental

The reversed-phase separations were performed by methods and on equipment described previously *(1,2)*. EIMS were obtained on equipment described previously *(23)*. The vanadyl etio and DPEP petroporphyrins were observed, when present, around m/z of 500. In addition, a plethora of peaks is also evident. This overwhelming continuum was characteristic of all fractions studied, and prevented us from using EIMS for any metal characterization other than vanadium petroporphyrin detection in the RP-HPLC fractions.

The separation procedures for the nickel carboxylate fraction isolated from Wilmington crude petroleum utilized both reversed-phase (ODS) and cyano normal phase HPLC techniques and details will be published elsewhere *(24)*. The FAB+ mass spectral methods will also be discussed elsewhere *(21)*. Model compounds for the studies were either purchased from Alfa Chemical Company, or synthesized by literature methods. The Gilsonite sample was separated by RP-HPLC-GFAA techniques and details will be reported elsewhere *(24)*.

Acknowledgements

We thank John J. Komlenic and Alejandro Izquierdo for experimental assistance, Dr. Geoffrey Eglinton of the University of Bristol for helpful suggestions, and Dr. Robert M. Carlson of Chevron Oil Field Research for the Gilsonite sample. The Lawrence Berkeley Laboratory studies were support by the Assistant Secretary of Fossil Energy, Division of Oil, Gas, and Shale technology, and the Bartlesville Project Office of the U.S. Department of Energy under contract DE-AC03-765F00098.

Literature Cited

(1) Fish, R.H.; Komlenic, J.J. *Anal. Chem.* 1984, 56, 510.
(2) Fish, R.H.; Komlenic, J.J.; Wines, B.K. *Anal. Chem.* 1984, 56, 2452.
(3) Boduszynski, M.M.; McKay, J.F.; Latham, D.R. *Assoc. of Asphalt Paving Tech.* 1980, 49, 123.
(4) Boduszynski, M.M. In "Chemistry of Asphaltenes." J.W. Bunger (ed.), *Adv. in Chem. Ser.* 1981, 195, 119.
(5) Reynolds, J.G.; Gallegos, E.J.; Fish, R.H.; Komlenic, J.J. Submitted to *Energy and Fuels* 1986.
(6) Dickson, F.E.; Kunesh, C.J.; McGinnis, E.L.; Petrakis, L. *Anal. Chem.* 1972, 44, 978.
(7) Dickson, F.E.; Petrakis, L. *Anal. Chem.* 1974, 44, 1129.
(8) Yen, T.F.; Boucher, L.J.; Dickie, J.P.; Tynan E.C.; Vaughan, G.B. J. Inst. Petrol. 1969, 55, 87.
(9) Yen, T.F. In "The Role of Trace Metals in Petroleum." T.F. Yen (ed.), Ann Arbor Sci., 1975, Ann Arbor, MI. Chap. 1, 1.
(10) McCormick, B.J.; Bellott, E.M. *Inorg. Chem.* 1970, 9, 1779.
(11) More, K.M.; Eaton, S.S.; Eaton, G.R. *J. Amer. Chem. Soc.* 1981, 103, 1087.
(12) Ocampo, R.; Callot, H.J.; Albrecht, P. *J. Chem. Soc., Chem. Comm.* 1985, 198.

(13) Blumer, M.; Synder, W.D. *Chem. Geol.* 1967, 2, 35.

(14) Blumer, M.; Rudrum, R. *J. Inst. of Petrol.* 1970, 56(548), 99.

(15) Johnson, J.V.; Britton, E.D.; Yost, R.A.; Quirke, J.M.E.; Cuesta, L.L. *Anal. Chem.* 1986, 58, 1325.

(16) Reynolds, J.G. *Liq. Fuels Tech.* 1985, 3(1), 73.

(17) Reynolds, J.G.; Biggs, W.R.; Fetzer, J.C. *Liq. Fuels Tech.* 1985, 3(4), 423.

(18) O'Laughlin, J.W. *J. of Liq. Chrom.* 1984, 7, 127.

(19) Reynolds, J.G.; Gallegos, E.J.; Fish, R.H. Manuscript in preparation, 1986.

(20) Seifert, W.K. *Progress in Chem. Org. Nat. Products* 1975, 32, 1.

(21) Gallegos, E.J.; Reynolds, J.G.; Fish, R.H. 33rd Annual Conference on Mass Spectrometry and Allied Topics, San Diego, 1985.

(22) Quirke, J.M.E.; Eglinton, G.; Maxwell, J.R. *J. Amer. Chem. Soc.* 1979, 101, 7693.

(23) Sundararaman, P.; Gallegos, E.J.; Baker, E.W.; Slayback, J.R.B.; Johnston, M.R. *Anal. Chem.* 1984, 56, 2552.

(24) Fish, R.H.; Reynolds, J.G.; Gallegos, E.J. Manuscript in preparation, 1986.

Figure Captions

Figure 1	Electron Impact Mass Spectrum for Cerro Negro Moderate Polar Fraction.
Figure 2	Electron Impact Mass Spectrum for Prudhoe Bay Low Polar Fraction.
Figure 3	HPLC-GFAA Profile for the Nickel Complexes from the Cyano Column Separation of the High Polar Reversed-Phase Fraction of Wilmington Crude Petroleum Extract.
Figure 4	Electron Impact Mass Spectra of Selected Nickel Model Compounds.
Figure 5	Electron Impact Mass Spectrum of Synthesized Nickel Naphthenates.
Figure 6	Electron Impact Mass Spectrum of the Cyano HPLC Column Purified Nickel Fraction from Wilmington Crude Petroleum Extract.
Figure 7	Positive Ion Fast Atom Bombardment Spectrum of Synthesized Nickel Naphthenates.
Figure 8	Positive Ion Fast Atom Bombardment Spectrum of Synthesized Nickel Naphthenates with TEA and Calcium Acetate.
Figure 9	Positive Ion Fast Atom Bombardment Spectrum of Cyano HPLC Column Purified Nickel Fraction from Wilmington Crude Petroleum Extract with TEA and Calcium Acetate.
Figure 10	Possible Carboxylic Acid Ligands for Nickel Complexes in the Cyano HPLC Column Purified Nickel Fraction from Wilmington Crude Petroleum.
Figure 11	RP-HPLC-GFAA Nickel Profile for a Gilsonite Sample Dissolved in THF.

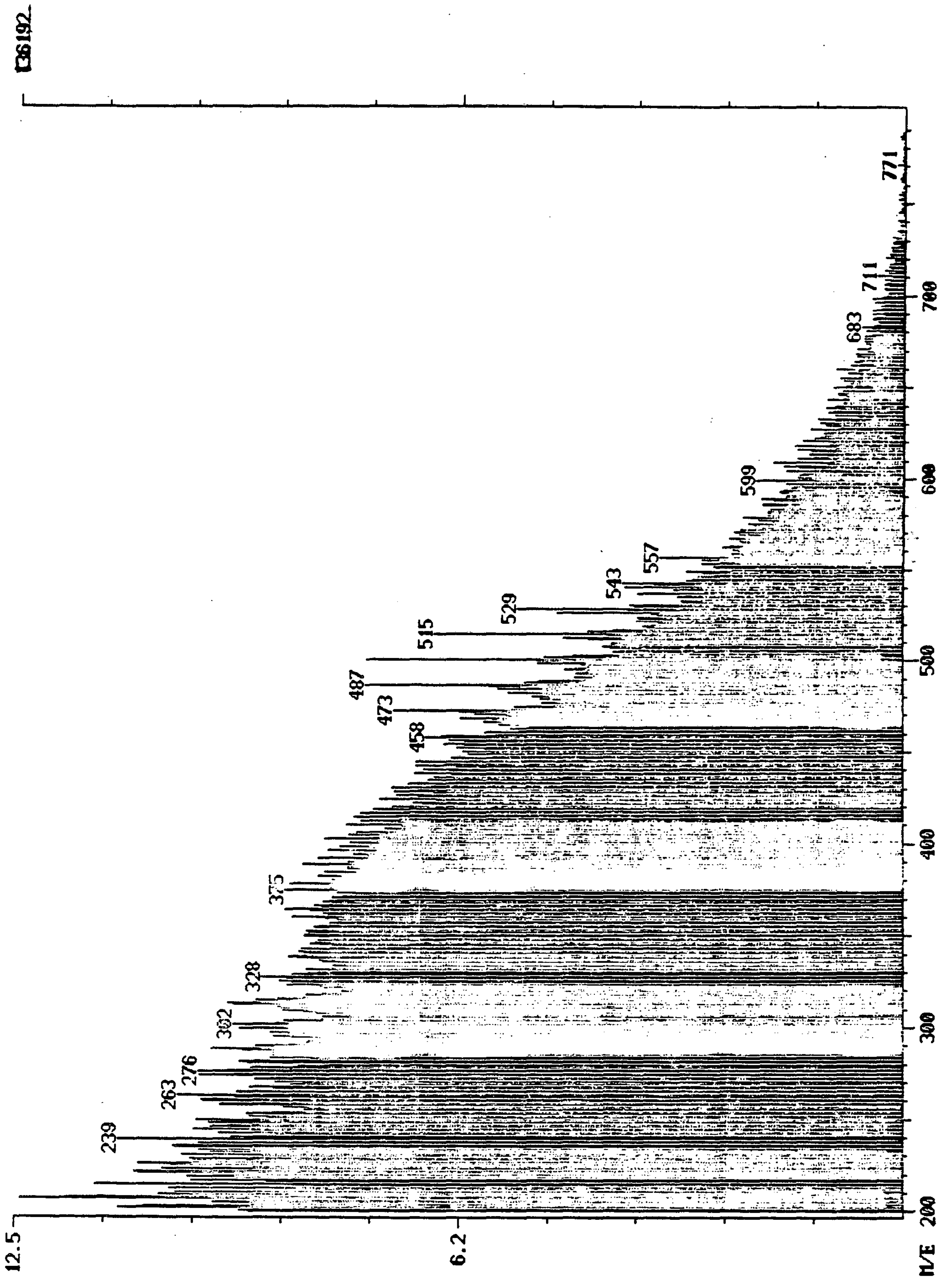

12.5
6.2
M/E
136192
200
300
400
500
600
700
239
263
276
302
328
375
458
473
487
515
529
543
557
599
683
711
771

Figure 1

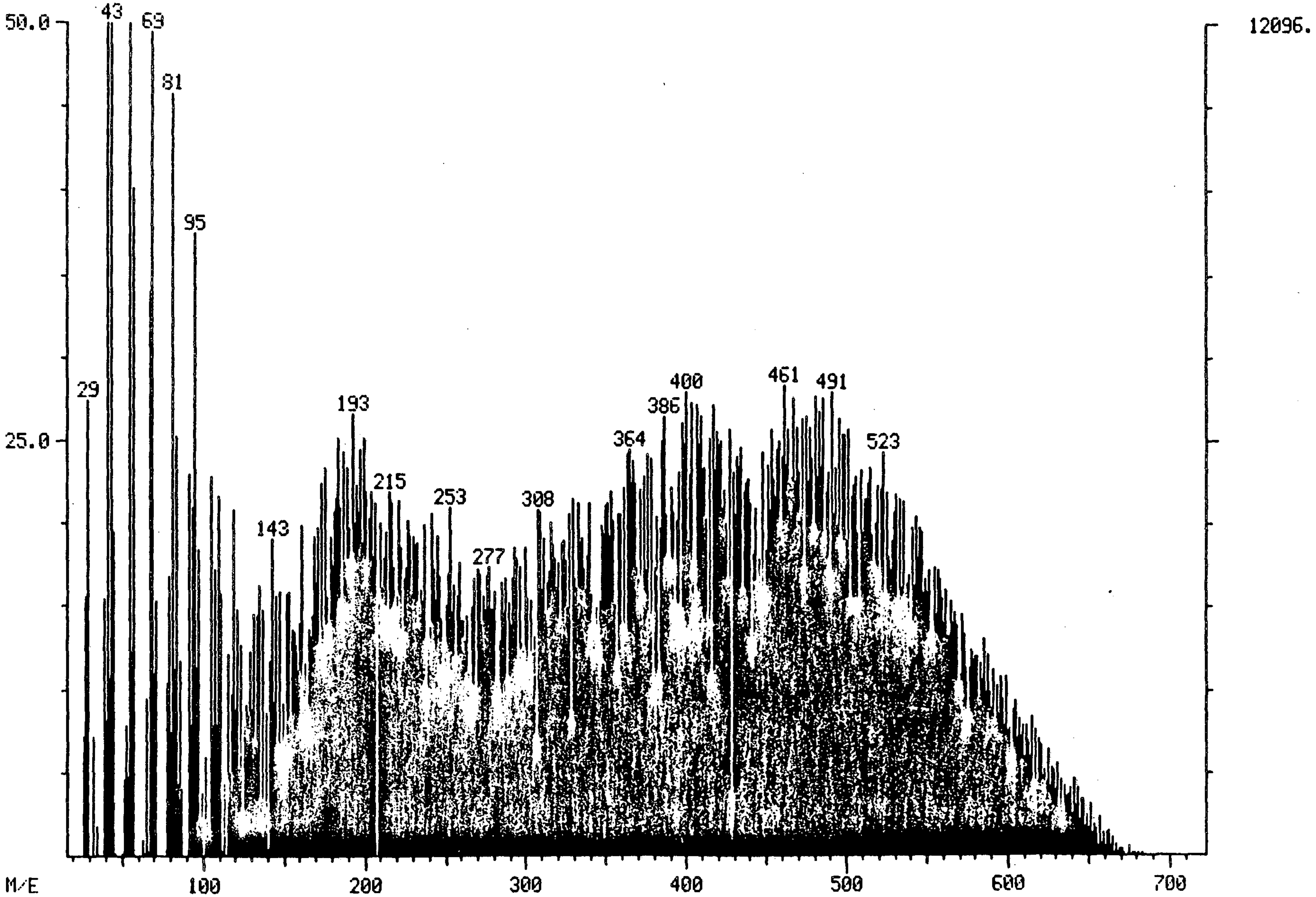

50.0
25.0
12096.
M/E
100
200
300
400
500
600
700
29
43
69
81
95
143
193
215
253
277
308
364
386
400
461
491
523

Figure 2

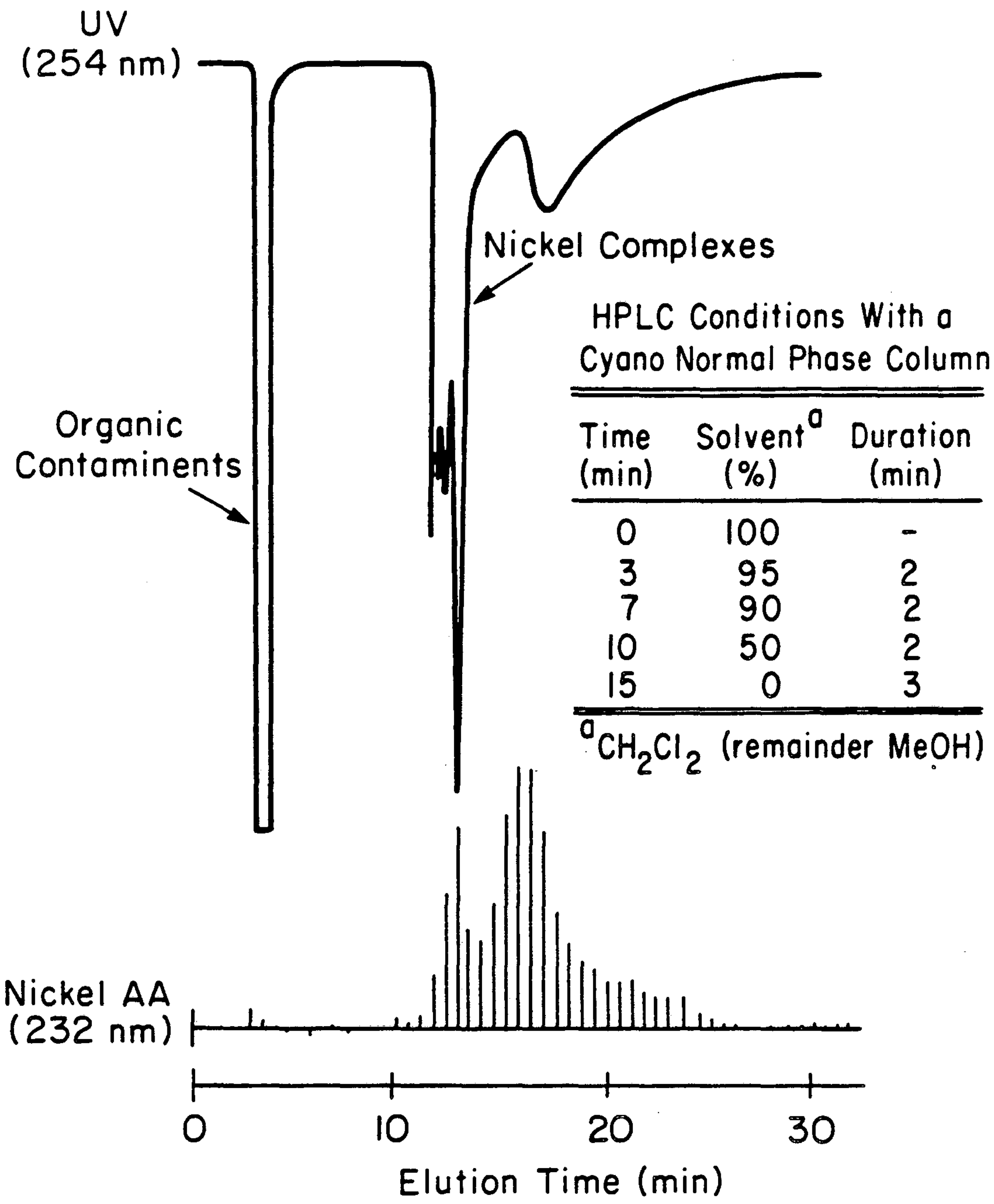

HPLC Conditions With a Cyano Normal Phase Column

Time (min)	Solvent^a (%)	Duration (min)
0	100	-
3	95	2
7	90	2
10	50	2
15	0	3

^{a} CH_2Cl_2 (remainder MeOH)

XBL 8610-3907

Figure 3

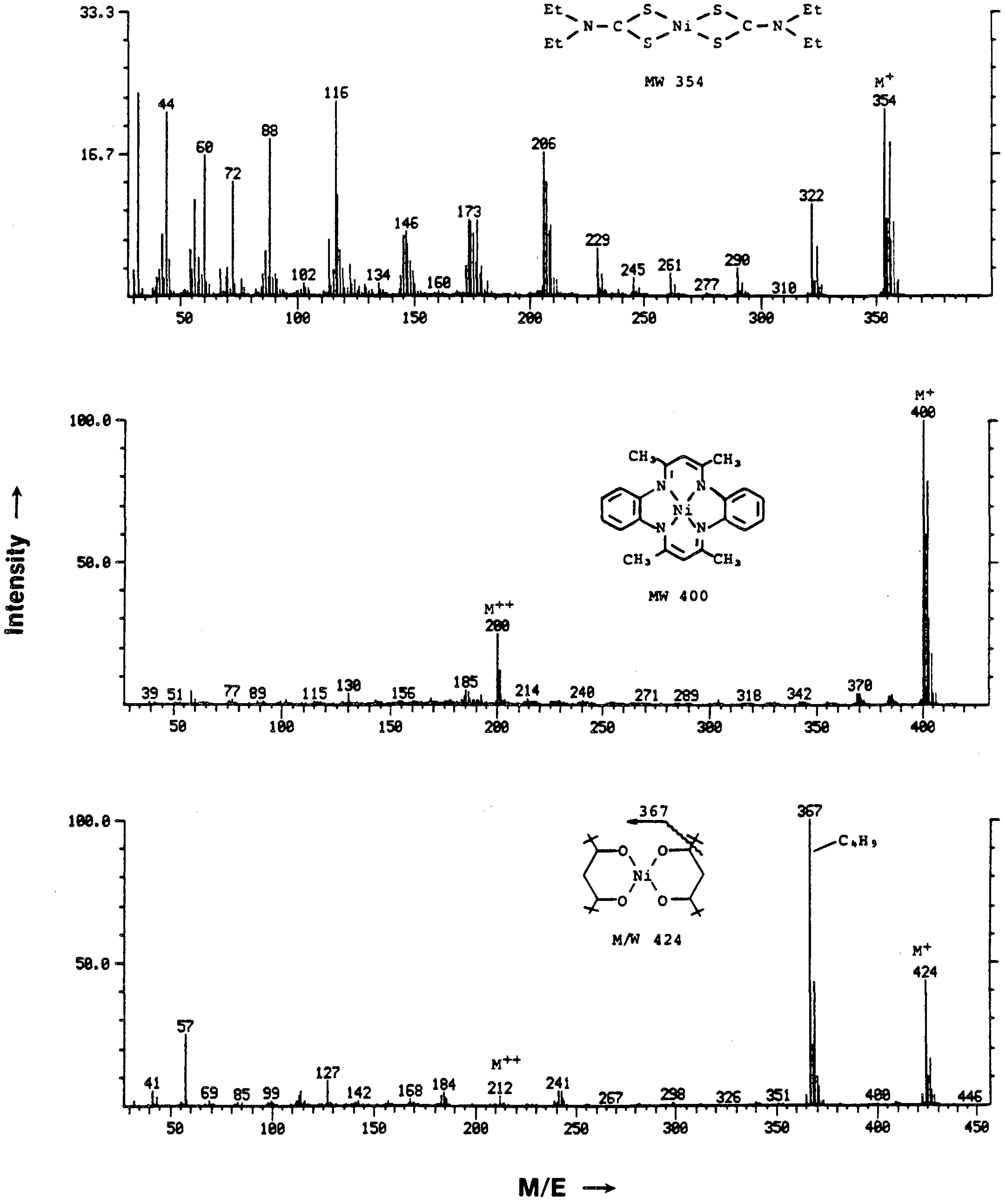

33.3
16.7
Et
N
C
S
Ni
MW 354
M+
354
44
60
72
88
102
116
134
146
160
173
206
229
245
261
277
290
310
322
50
100
150
200
250
300
350
100.0
50.0
M+
400
CH3
N
Ni
MW 400
M++
200
39
51
77
89
115
130
156
185
214
240
271
289
318
342
370
50
100
150
200
250
300
350
400
100.0
50.0
367
C4H9
O
Ni
M/W 424
M+
424
57
41
69
85
99
127
142
168
184
M++
212
241
267
298
326
351
400
446
50
100
150
200
250
300
350
400
450
Intensity →
M/E →

Figure 4

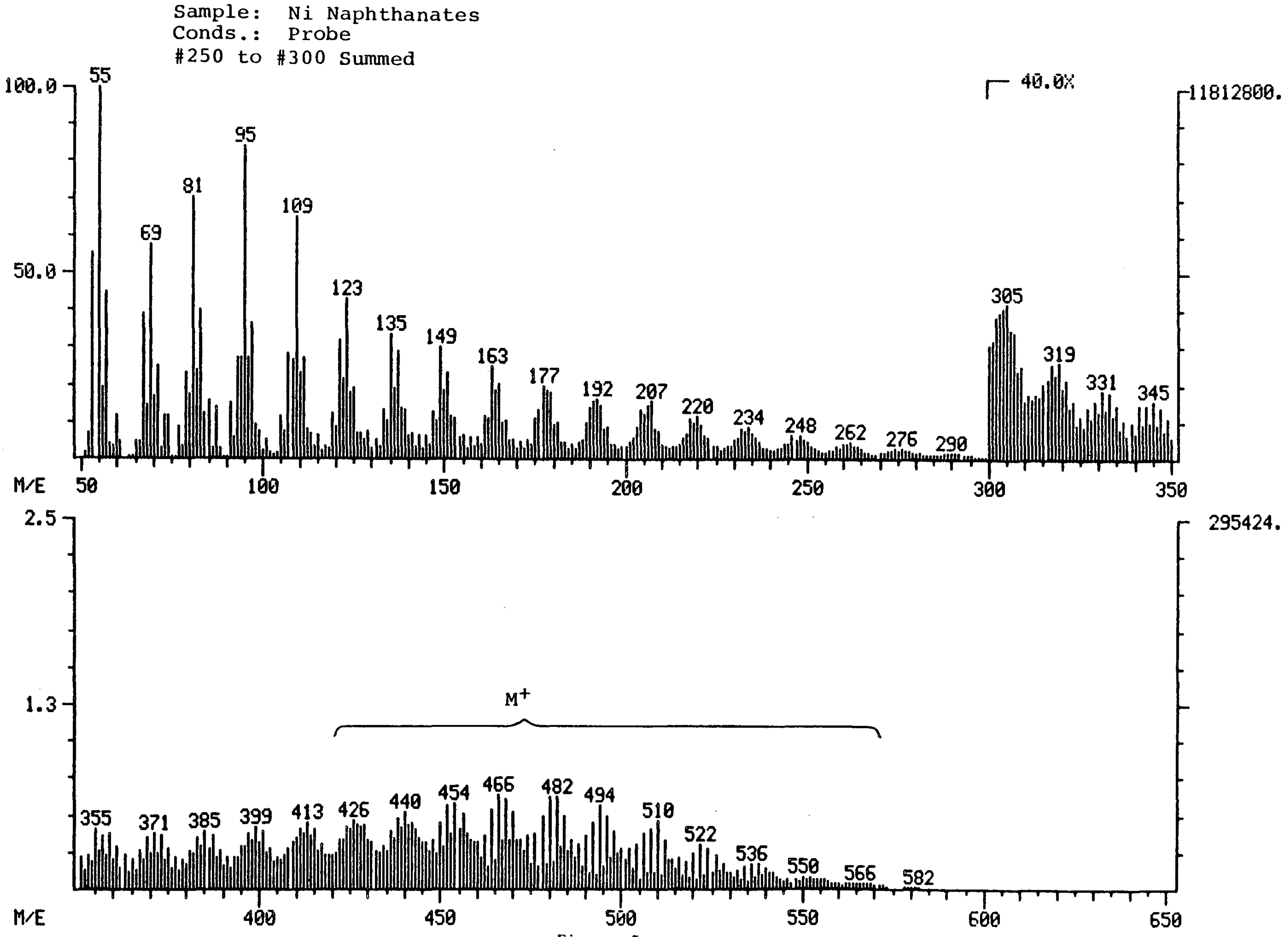
Sample: Ni Naphthanates
Conds.: Probe
#250 to #300 Summed
100.0
50.0
55
69
81
95
109
123
135
149
163
177
192
207
220
234
248
262
276
290
305
319
331
345
40.0%
11812800.
M/E
50
100
150
200
250
300
350
2.5
1.3
295424.
M+
355
371
385
399
413
426
440
454
466
482
494
510
522
536
550
566
582
M/E
400
450
500
550
600
650

Figure 5

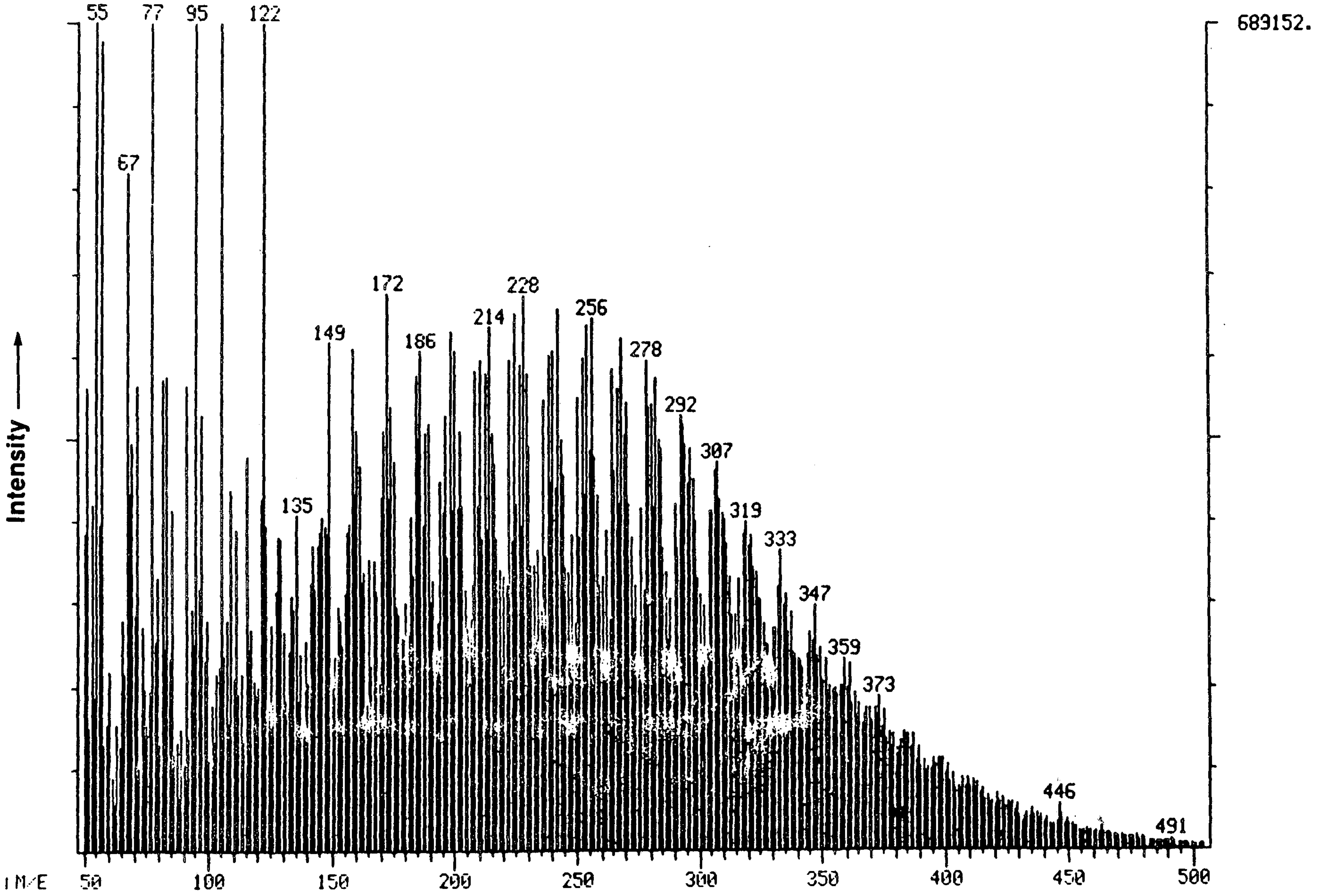
55
77
95
122
683152.
67
172
228
214
256
149
186
278
292
307
135
319
333
347
359
373
446
491
Intensity
M/E
50
100
150
200
250
300
350
400
450
500

Figure 6

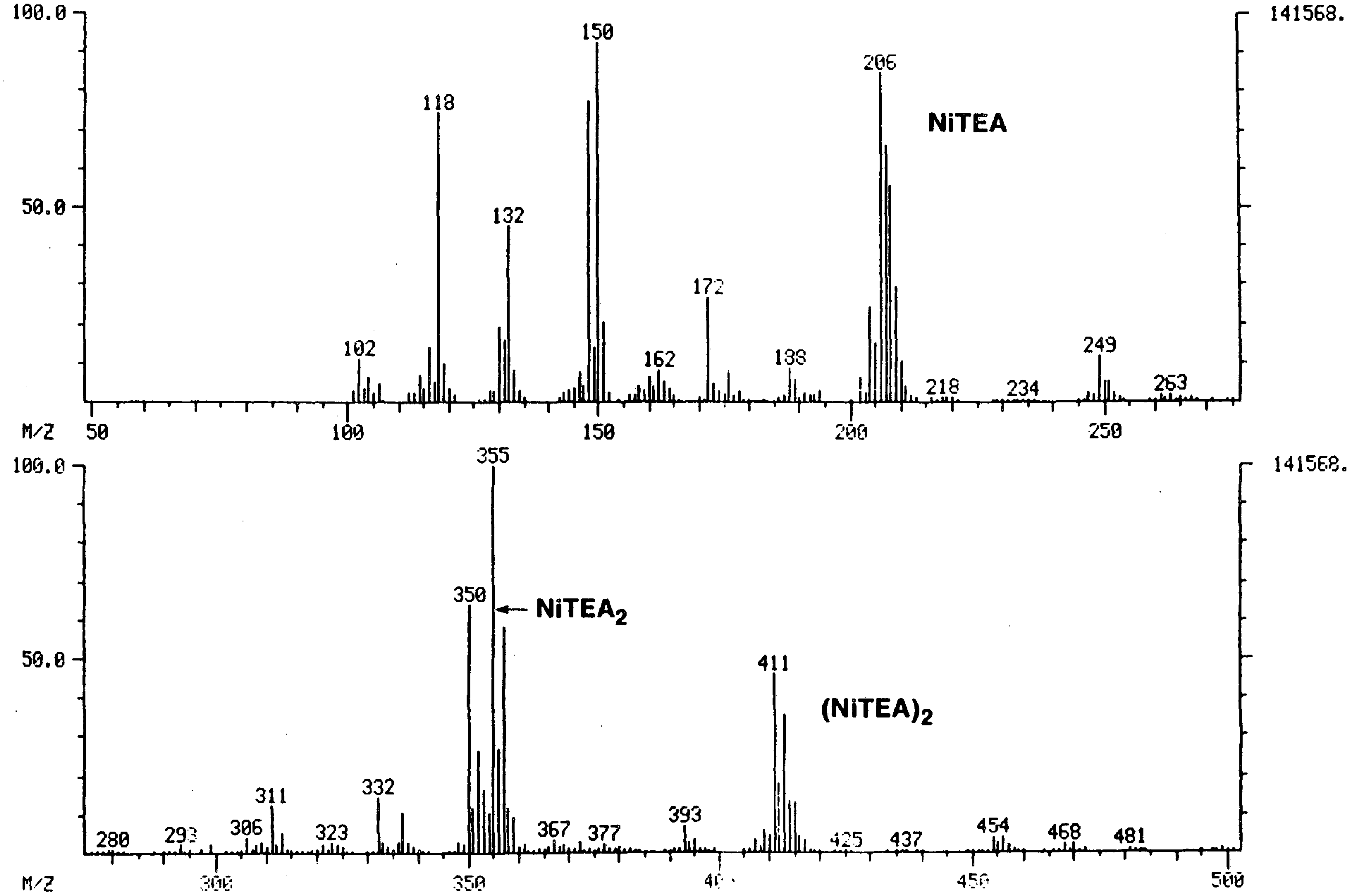
100.0
50.0
141568.
102
118
132
150
162
172
188
206
218
234
249
263
NiTEA
M/Z
50
100
150
200
250
100.0
50.0
141568.
280
293
306
311
323
332
350
355
NiTEA$_2$
367
377
393
411
(NiTEA)$_2$
425
437
454
468
481
M/Z
300
350
400
450
500

Figure 7

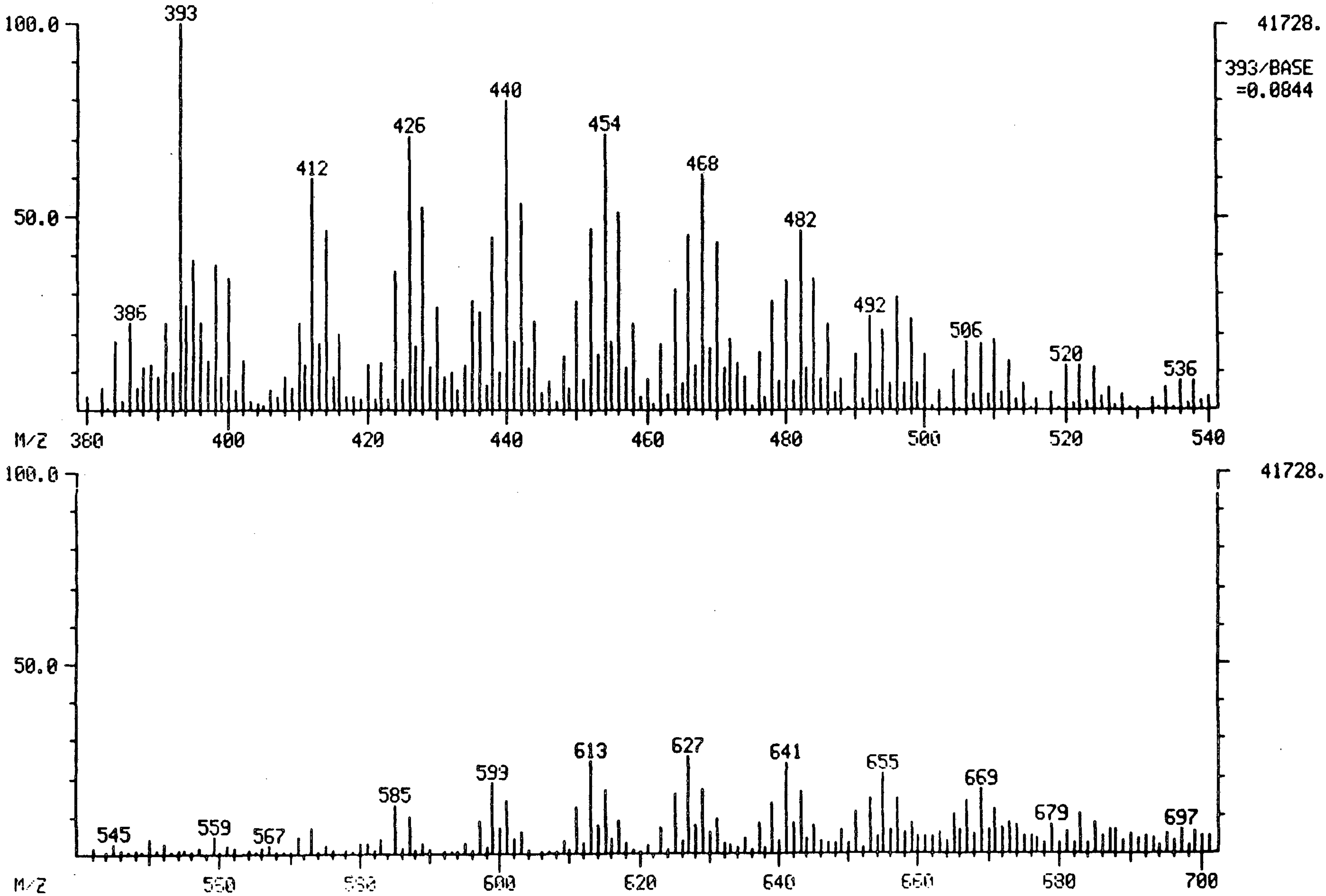
100.0
50.0
393
440
426
454
412
468
482
386
492
506
520
536
41728.
393/BASE
=0.0844
M/Z
380
400
420
440
460
480
500
520
540
100.0
50.0
41728.
545
559
567
585
593
613
627
641
655
669
679
697
M/Z
560
580
600
620
640
660
680
700

Figure 8

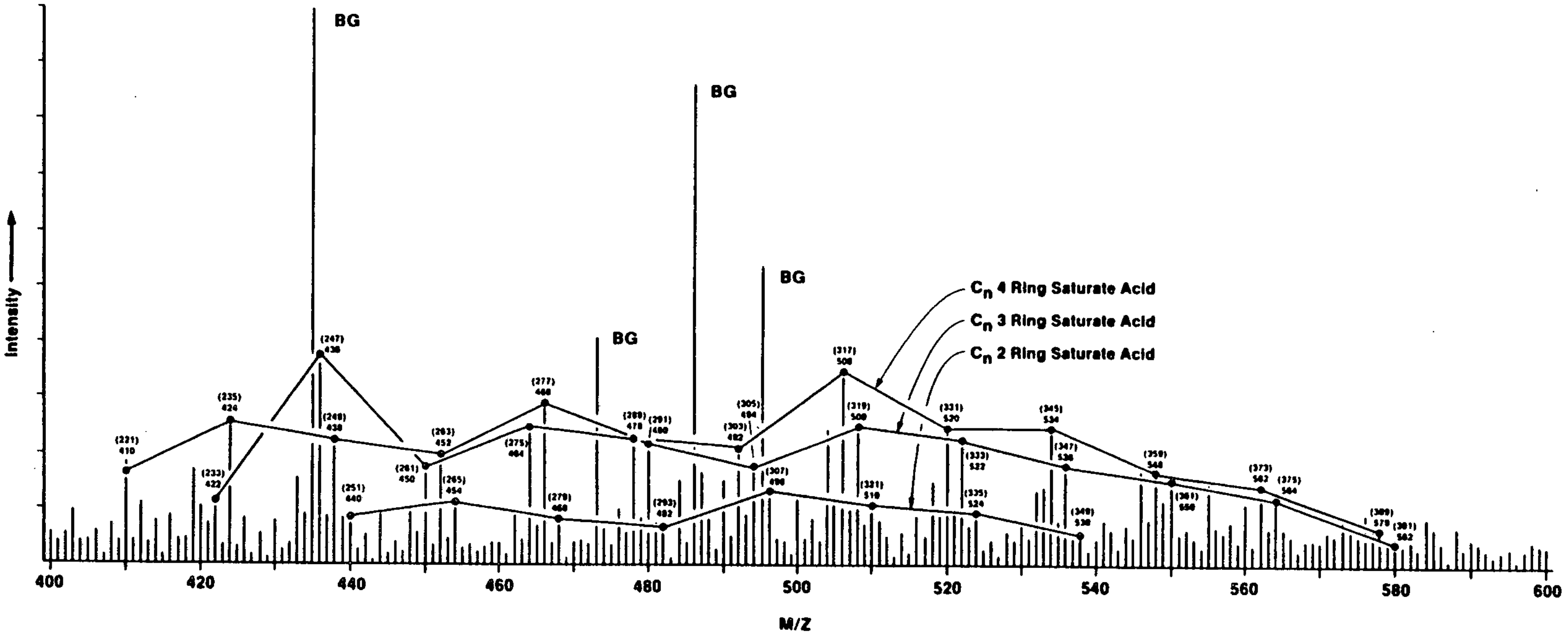
Intensity
BG
BG
BG
BG
Cn 4 Ring Saturate Acid
Cn 3 Ring Saturate Acid
Cn 2 Ring Saturate Acid
(221) 410
(233) 422
(235) 424
(247) 436
(249) 438
(251) 440
(261) 450
(263) 452
(265) 454
(275) 464
(277) 466
(279) 468
(289) 478
(291) 480
(293) 482
(303) 492
(305) 494
(307) 496
(317) 506
(319) 508
(321) 510
(331) 520
(333) 522
(335) 524
(345) 534
(347) 536
(349) 538
(359) 548
(361) 550
(373) 562
(375) 564
(389) 578
(391) 580
400
420
440
460
480
500
520
540
560
580
600
M/Z

Figure 9

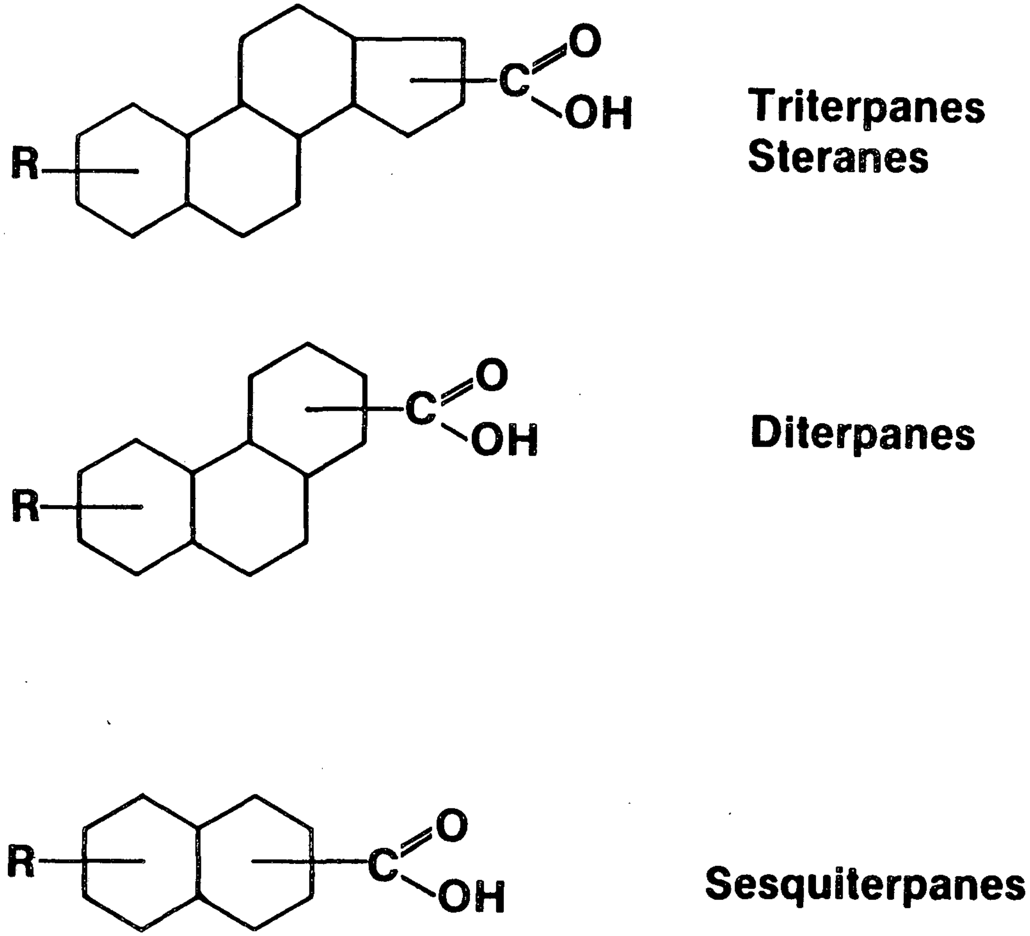
R
C
O
OH
Triterpanes
Steranes
R
C
O
OH
Diterpanes
R
C
O
OH
Sesquiterpanes

Figure 10

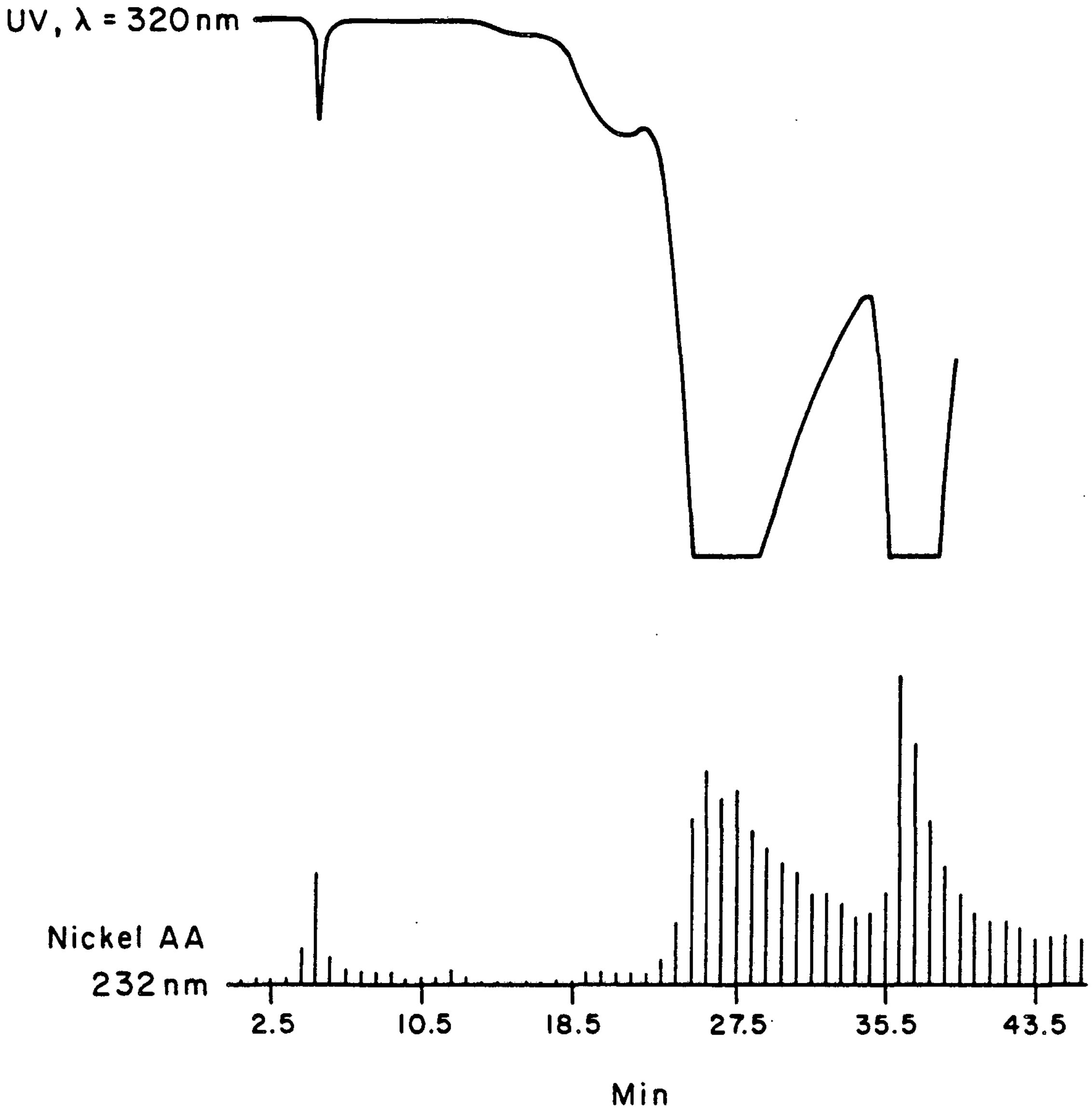
UV, λ = 320nm
Nickel AA
232nm
2.5
10.5
18.5
27.5
35.5
43.5
Min
XBL 864-1337

Figure 11

LAWRENCE BERKELEY LABORATORY
TECHNICAL INFORMATION DEPARTMENT
UNIVERSITY OF CALIFORNIA
BERKELEY, CALIFORNIA 94720